

## Analysis of Deep-level Mine Design Problems Using the MINSIM-D Boundary Element Program

J.A.L. NAPIER\* and S.J. STEPHANSEN\*\*

\*Chamber of Mines of South Africa Research Organization, Johannesburg

\*\*General Mining Union Corporation Group Information Services, Bedfordview, South Africa

Computer programs which rely on the assumption of linear, elastic rockmass behaviour have been used routinely for many years in the South African mining industry to determine the stresses arising in the vicinity of mining excavations.

A description is given of the theoretical background and novel solution techniques used in the recently developed MINSIM-D boundary element program. Features of the program include the ability to analyse multiple interacting reef planes at arbitrary orientation to one another, slippage on fault planes and the effects of backfill placement in mined areas. Incremental mining sequences can be modelled, and digitizer and front-end routines have been written to assist in the capture of mining outlines and general problem specifications.

A brief indication is given of design problems for which MINSIM-D is appropriate, as well as some future extensions of the system.

### Introduction

Applications of boundary element techniques to the analysis of underground stress problems have been pursued vigorously during the last two decades with the increasing availability of high speed computers. In the South African gold mining industry, particular impetus was given to the exploitation of this approach when it became apparent that the rockmass could be approximated as an isotropic elastic continuum.<sup>(1)</sup> The analysis of narrow, tabular deposits associated with many gold and coal mines proved to be amenable to an elegant variation of the boundary element method referred to by Salamon as the 'face element' principle<sup>(2)</sup> and currently known as the 'displacement discontinuity' method.<sup>(3), (4)</sup>

In this method all stresses in the medium are determined by the relative movement between the roof and the floor of the exca-

vations - the so-called displacement discontinuity. The displacement discontinuity is a vector quantity whose components are conveniently resolved along two axes in the plane of the excavation and a third axis normal to the plane of the excavation. The components in the plane are termed 'rides', and the normal component is termed the 'closure'. The rides represent the tangential movement of the roof relative to the floor, and the closure represents the movement of the roof towards the floor of the excavation.

All components will, in general, vary over the excavation and must be solved to satisfy specified stress boundary conditions in the excavation. The first solutions of this kind were obtained, for complex mining outlines, by means of specially constructed electrolytic and resistance analogue compu-

ters.(5) Subsequently, Deist(6), (7) produced a digital computer program (MINSIM) which enabled mining outlines on a single reef plane to be described by an array of 64 x 64 grid elements, each of which was designated as 'mined' or 'solid'. The same approach has been used as the basis for a number of independently developed programs.(4), (8), (9), (10)

Successive versions of MINSIM-D have been developed at the Chamber of Mines Research Organization. This paper describes some of the enhancements which comprise the current system, referred to as MINSIM-D. These include a novel method of solution iteration, improvements to the solution accuracy and additional aids for preparing input data directly from mine plans.

### Tabular excavation modelling

The analysis of thin, sheet-like excavations made in tabular deposits can be accomplished by dividing the mined area into a regular array of elements. In particular if a square element of side  $g$  is centred at point  $Q$ , as shown in Figure 1, and if the displacement discontinuity components,  $S_k$ , are constant over the element, the stresses,  $\tau_{ij}$ , at point  $P$  in an isotropic elastic medium were shown by Rongved(3) and Salamon(2) to be given by relations of the form

$$\tau_{ij}(P) = (E/8\pi(1-\nu^2)g)M_{ijk}(P,Q) S_k(Q) \quad (1)$$

where point  $P$  has coordinates  $(x, y, z)$  relative to point  $Q$ .  $E$  and  $\nu$  are the Young's modulus and Poisson's ratio of the medium. The components  $M_{ijk}$  are termed 'influence coefficients' or 'kernels', and summation over the free index  $k$  is assumed implicitly.

Similarly, the displacements,  $u_i$ , at point  $P$  are given by relations of the form

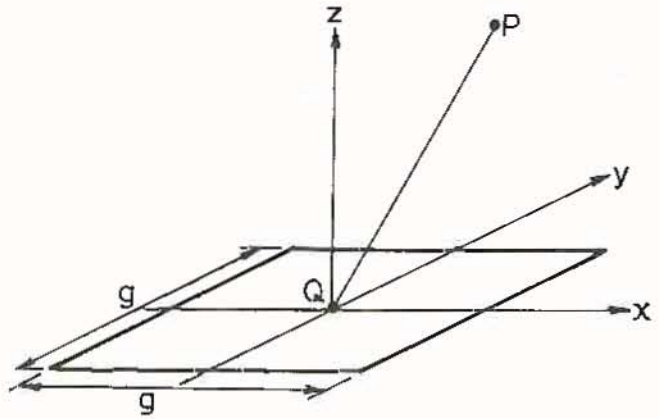


FIGURE 1. Local axis system,  $x, y, z$  erected on a square element of side  $g$

$$u_i(P) = (1/8\pi(1-\nu))N_{ik}(P,Q)S_k(Q) \quad (2)$$

where  $N_{ik}$  are a second set of kernels.

The kernel components  $M_{ijk}(P,Q)$  and  $N_{ik}(P,Q)$  are functions of the dimensionless coordinates  $X = x/g$ ,  $Y = y/g$ ,  $Z = z/g$  between points  $P$  and  $Q$  and of the Poisson's ratio,  $\nu$ . They can be expressed in terms of the Newtonian potential function,  $I$ , and its derivatives, given by Equation(3).(3)

$$I = \int_{-g/2}^{+g/2} \int_{-g/2}^{+g/2} [(x-\xi)^2 + (y-\eta)^2 + z^2]^{-1/2} d\xi d\eta$$

$$= \sum_{e_1, e_2} e_1 e_2 [B \log(A+R) + A \log(B+R) - z \arctan(AB/zR)] \quad (3)$$

where  $A = x - e_1 g/2$   
 $B = y - e_2 g/2$   
 $R = \sqrt{A^2 + B^2 + z^2}$   
 $e_1 = -1, +1$  ;  $e_2 = -1, +1$  .

It should be noted that only nine of the stress kernel components,  $M_{ijk}$ , and five of the displacement kernel components,  $N_{ik}$ , are independent functions.

### Solution technique

Actual mining problems are solved by superimposing a grid of square elements over the

mined areas. In practice, planar groups of 64 x 64 elements (termed 'windows') are found to provide a sufficiently detailed resolution for most excavation outlines. (6), (7) Each element in such a window is assigned a status of 'mined' or 'solid'. The total stress,  $\tau_{ij}$ , induced at a mined element, P, is computed by summing Equation (1) over the complete set of defined elements, Q. Clearly, if the boundary stresses are stipulated at each mined element, this set of equations can be solved for the appropriate displacement discontinuity distribution in each excavation.

A mining problem generally involves several interacting windows of 64 x 64 elements. The normal components,  $T_x$ ,  $T_y$ ,  $T_z$ , of the total stress tensor acting at the centre of a particular element, P, can be expressed by a vector equation of the form

$$\begin{bmatrix} T_x \\ T_y \\ T_z \end{bmatrix} = C \begin{bmatrix} M_x S_x \\ M_y S_y \\ M_z S_z \end{bmatrix} + \begin{bmatrix} P_x \\ P_y \\ P_z \end{bmatrix} + \begin{bmatrix} E_x \\ E_y \\ E_z \end{bmatrix} + \begin{bmatrix} \bar{E}_x \\ \bar{E}_y \\ \bar{E}_z \end{bmatrix}, \quad (4)$$

where  $C = E/(8\pi(1-\nu^2)g)$  (5)

In Equation (4),  $M_x$ ,  $M_y$ ,  $M_z$  represent the 'self-effect' stress kernels which arise when point P coincides with point Q in Equation (1). The x and y axes are in the plane of the excavation and the z axis is normal to this plane.

Specifically, it can be shown that

$$\begin{bmatrix} M_x \\ M_y \\ M_z \end{bmatrix} = 8\sqrt{2} \begin{bmatrix} 1 - \frac{\nu}{2} \\ 1 - \frac{\nu}{2} \\ 1 \end{bmatrix} \quad (6)$$

$S_x$  and  $S_y$  represent the 'ride' components and  $S_z$  the 'closure' component of the displacement discontinuity vector.  $P_x$ ,  $P_y$ ,  $P_z$  are the primitive stress components acting on the element. It is convenient to partition the induced stress arising at element P into two vectors:  $E_x$ ,  $E_y$ ,  $E_z$  represent the components of induced stress at P due to all mined elements within the window containing element P and  $\bar{E}_x$ ,  $\bar{E}_y$ ,  $\bar{E}_z$  represent the induced stresses at P due to all mined elements external to the window containing P.

The left hand side of Equation (4) represents the total stress vector acting on element P. This is required to be zero in open excavation zones but may be equated to the reaction stress arising from the compression of artificial support or backfill material. To accommodate a non-linear reaction stress in Equation (4), it is convenient to implement a novel iterative scheme proposed by Ryder. (11) The right hand side of Equation (4) is considered to be a linear function of  $S_x$ ,  $S_y$ ,  $S_z$  with an intercept vector, I, whose components  $I_x$ ,  $I_y$ ,  $I_z$  are defined by

$$I = \begin{bmatrix} I_x \\ I_y \\ I_z \end{bmatrix} = \begin{bmatrix} P_x \\ P_y \\ P_z \end{bmatrix} + \begin{bmatrix} E_x \\ E_y \\ E_z \end{bmatrix} + \begin{bmatrix} \bar{E}_x \\ \bar{E}_y \\ \bar{E}_z \end{bmatrix} \quad (7)$$

Iteration is performed by accelerating the current estimate of the intercept vector, I, rather than the solution variables  $S_x$ ,  $S_y$ ,  $S_z$ . The new estimate of the intercept vector is

$$I_{new} = I_{old} + \omega (I - I_{old}), \quad (8)$$

where  $\omega$  is the over-relaxation parameter

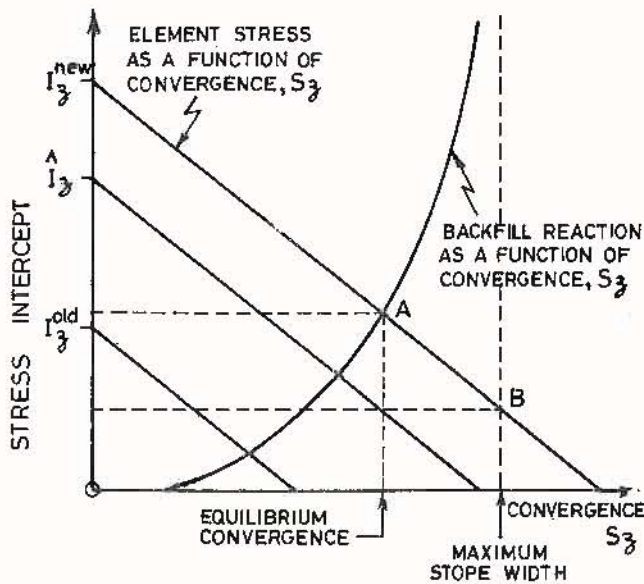


FIGURE 2. Intersection of element stress line with a backfill reaction curve at point A or total closure limit at point B

which is used in the iterative solution. In practice  $w$  should be chosen to fall between 1 and 2; a value of 1.5 yields acceptable solutions within approximately 15 iterations for a single 64 x 64 window.

The components of  $I_z^{new}$  are substituted into Equation (4), which is then solved for  $S_x$ ,  $S_y$  and  $S_z$  by equating the right hand side to the required boundary condition or reaction function. This is illustrated for the z-component in Figure 2.

The residual error at each element is computed from the inner product,

$$R = \sqrt{[(I - I^{old}) \cdot (I - I^{old})]} \quad (9)$$

The maximum residual,  $R_{max}$ , arising during a complete pass of all mined elements in a given window is noted and compared to the desired stress tolerance for iterative convergence. This is usually chosen to be of the order of 1/2 per cent of the maximum primitive stress.

Experience with this method of iteration has indicated that it is robust and performs with similar efficiency to schemes involving direct over-relaxation of the solution

variables. It is particularly convenient for controlling iteration when total closure (roof and floor contact) occurs.

### Treatment of total closure

Extensive excavation of tabular gold deposits often results in total closure of parts of the mined out areas. The total normal stress  $T_z$  then corresponds to point B in Figure 2.

The shear stresses  $T_x$  and  $T_y$  and the ride components  $S_x$  and  $S_y$  are indeterminate unless the unrealistic assumption is made that there is no frictional resistance to sliding once hangingwall and footwall contact is established. However, it is possible to obtain a convenient and smooth estimate of the ride distribution if a plausible assumption can be made about the ratios of the ride components to the normal closure at the onset of total closure. These ratios are estimated by rewriting Equation (4) in the form

$$\begin{bmatrix} T_x \\ T_y \\ T_z \end{bmatrix} = \begin{bmatrix} a S_x \\ b S_y \\ c S_z \end{bmatrix} + \begin{bmatrix} P_x \\ P_y \\ P_z \end{bmatrix} + \begin{bmatrix} \bar{E}_x \\ \bar{E}_y \\ \bar{E}_z \end{bmatrix} \quad (10)$$

where

$$\begin{bmatrix} a S_x \\ b S_y \\ c S_z \end{bmatrix} = C \begin{bmatrix} M_x S_x \\ M_y S_y \\ M_z S_z \end{bmatrix} + \begin{bmatrix} E_x \\ E_y \\ E_z \end{bmatrix}$$

is the induced stress due to mining within the current window. This is represented by suitable 'macro' kernel components  $a$ ,  $b$ ,  $c$  which reflect the overall displacement discontinuity pattern within the window. If there were no closure restrictions the

total rides and convergences  $\bar{S}_x, \bar{S}_y, \bar{S}_z$  in Equation (10) would be given by

$$\begin{bmatrix} a \bar{S}_x \\ b \bar{S}_y \\ c \bar{S}_z \end{bmatrix} + \begin{bmatrix} P_x \\ P_y \\ P_z \end{bmatrix} + \begin{bmatrix} \bar{E}_x \\ \bar{E}_y \\ \bar{E}_z \end{bmatrix} = 0 \quad (11)$$

The assumption is then made that the actual rides and convergence are proportional to  $\bar{S}_x, \bar{S}_y$  and  $\bar{S}_z$ , i.e.

$$\begin{bmatrix} S_x \\ S_y \\ S_z \end{bmatrix} = \gamma \begin{bmatrix} \bar{S}_x \\ \bar{S}_y \\ \bar{S}_z \end{bmatrix} \quad (12)$$

At total closure, the convergence,  $S_z$ , is equal to the known slope width and the total normal stress,  $T_z$ , can be determined from Equation (4). Using the third member of Equations (10), (11) and (12), the proportionality constant,  $\gamma$ , can be shown to be

$$\gamma = 1 - T_z / (P_z + E_z) \quad (13)$$

From the first and second members of Equations (4), (10), (11) and (12), provisional ride components  $\hat{S}_x$  and  $\hat{S}_y$  are given by

$$\begin{bmatrix} M_x \hat{S}_x \\ M_y \hat{S}_y \end{bmatrix} = -\gamma \begin{bmatrix} P_x + \bar{E}_k \\ P_y + \bar{E}_y \end{bmatrix} - \begin{bmatrix} E_x \\ E_y \end{bmatrix} \quad (14)$$

The ride components  $\hat{S}_x, \hat{S}_y$  are employed in Equation (4) to find the total shear stresses  $\hat{T}_x, \hat{T}_y$  acting on the element. If the resultant shear stress,  $\tau$ , exceeds the specified frictional resistance,  $\rho$ , sliding

is allowed to occur until the resultant out of balance shear stress is zero. Specifically, the resultant shear stress is

$$\tau = \sqrt{[\hat{T}_x^2 + \hat{T}_y^2]} \quad (15)$$

If the frictional resistance to sliding is  $\rho$  and  $\tau > \rho$ , then the rides are adjusted to the final values

$$\begin{bmatrix} S_x \\ S_y \end{bmatrix} = \begin{bmatrix} \hat{S}_x \\ \hat{S}_y \end{bmatrix} - \left( \frac{\tau - \rho}{\tau} \right) \begin{bmatrix} T_x / M_x \\ T_y / M_y \end{bmatrix} \quad (16)$$

Figure 3 illustrates the application of the total closure algorithm to the case of a rectangular, 6 400 m x 1 000 m excavation with a limited slope width of 1 metre located at a depth of 3 000 m. The major axis of the excavation is horizontal and the minor axis dips at 30 degrees. The vertical primitive stress is assumed to be directly proportional to the depth (0,027 MPa/m) and the horizontal primitive stress equal to half the vertical stress. A Young's modulus of 70 000 MPa and a Poisson's ratio of 0,2 were used. The ride values along the central dip section are plotted in Figure 3

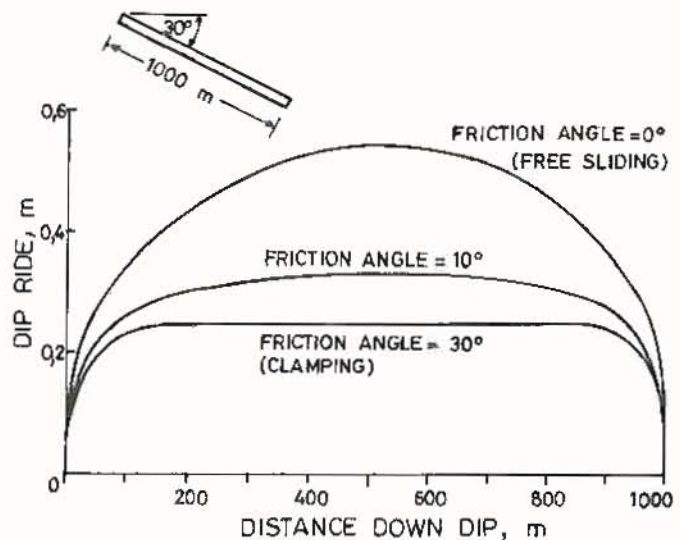


FIGURE 3. Ride values along the dip section of a parallel sided excavation in which total closure has occurred

for assumed contact friction angles of 0°, 10° and 30° between hangingwall and the footwall. At 0°, free sliding occurs with a maximum ride of 0,540 m, whereas at 30° clamping occurs yielding a uniform ride of 0,248 m at points of contact. In this case the ratio of ride to normal convergence corresponds to the ratio of the primitive shear and normal stresses in the plane of the excavation, as suggested by Salamon.(12)

### Partially mined elements

It has been shown by Ryder(13) that the use of constant displacement discontinuity elements leads to an over-estimation of the solution values. For two dimensional slits the numerical values can be made to agree with theoretical solutions if the excavation size is reduced by 1/4 of a grid unit at each edge. In addition to the 1/4 grid adjustment, excavation boundaries will generally not correspond to integral element boundaries.

Partially mined elements can be treated by adjusting the self-effect kernels which are applied at these elements. For a two dimensional slit in which generalized plane strain exists in the x-coordinate direction, it can be shown by integrating the Newtonian potential, I, given by Equation (3) in the x direction, that the appropriate self-effect stress components are given by

$$\begin{bmatrix} \tau_{xx}^{\circ} \\ \tau_{yy}^{\circ} \\ \tau_{zz}^{\circ} \\ \tau_{yz}^{\circ} \\ \tau_{zx}^{\circ} \\ \tau_{xy}^{\circ} \end{bmatrix} = 8 C \begin{bmatrix} 0 & 0 & 2\nu \\ 0 & 0 & 1 \\ 0 & 0 & 1 \\ 0 & 1 & 0 \\ 1-\nu & 0 & 0 \\ 0 & 0 & 0 \end{bmatrix} \begin{bmatrix} S_x \\ S_y \\ S_z \end{bmatrix} \quad (17)$$

where C is given by Equation (5).

The corresponding three dimensional self-effect matrix is

$$\begin{bmatrix} \tau_{xx}^{\circ} \\ \tau_{yy}^{\circ} \\ \tau_{zz}^{\circ} \\ \tau_{yz}^{\circ} \\ \tau_{zx}^{\circ} \\ \tau_{xy}^{\circ} \end{bmatrix} = 8\sqrt{2} C \begin{bmatrix} 0 & 0 & \nu + 1/2 \\ 0 & 0 & \nu + 1/2 \\ 0 & 0 & 1 \\ 0 & 1 - \frac{\nu}{2} & 0 \\ 1 - \frac{\nu}{2} & 0 & 0 \\ 0 & 0 & 0 \end{bmatrix} \begin{bmatrix} S_x \\ S_y \\ S_z \end{bmatrix} \quad (18)$$

The adjustment which must be added to each self-effect kernel in Equation (17) can be demonstrated to be given by the proportional matrix,

$$A = \alpha C \begin{bmatrix} 0 & 0 & 2\nu \\ 0 & 0 & 1 \\ 0 & 0 & 1 \\ 0 & 1 & 0 \\ 1-\nu & 0 & 0 \\ 0 & 0 & 0 \end{bmatrix} \quad (19)$$

where the proportionality constant,  $\alpha$ , is given by(13)

$$\alpha = 2\pi (1-m)/m \quad (20)$$

and m is the fraction of the element which is mined. For a fully mined element  $m = 1$  and  $\alpha = 0$ . As the fraction mined tends to zero (i.e. the element becomes solid),  $\alpha \rightarrow \infty$ , which implies that the element becomes infinitely stiff. By applying the three dimensional kernels of Equations (1) and (18) to the two dimensional plane strain geometry implied by Equation (17), it can be shown that the self-effect adjustments applied to Equation (18) are also given by Equation (19).

Assuming that the mining boundary in a given element is in fact at an angle  $\theta$  relative to the x-direction and that local plane

strain conditions exist parallel to the boundary, the self-effect adjustments of Equation (19) are appropriate for an axis system  $x', y'$  in which  $x'$  is parallel to the boundary. The general adjustment is then obtained by rotating these stress components to the required  $x, y$  system. The rotated matrix is given by

$$A = \alpha C \begin{bmatrix} 0 & 0 & p^2 + 2vq^2 \\ 0 & 0 & q^2 + 2vp^2 \\ 0 & 0 & 1 \\ -vpq & 1-vp^2 & 0 \\ 1-vq^2 & -vpq & 0 \\ 0 & 0 & -(1-2v)pq \end{bmatrix} \quad (21)$$

where  $p = \sin \theta$ ,  $q = \cos \theta$ .

### Influence lumping and kernel table storage

Direct computation of the induced stress components arising at a particular element of a  $64 \times 64$  window, due to all mined elements within the window, requires up to 4 095 cross influences to be computed. A single iteration pass of all elements in the window therefore involves the potential computation of 16 million influence varieties. This computational effort can be reduced by grouping the window elements into  $2 \times 2$ ,  $4 \times 4$  and  $8 \times 8$  units, termed 'lumps' by Deist.<sup>(7)</sup> Influences are computed between lumps of the same size with the proviso that a specified minimum number of lump units, referred to as the number of lump shells,  $L$ , separates any receiving and sending lump. This scheme reduces the number of cross influences per iteration by the factors shown in Table 1.

In practice, it is found that the solution accuracy is acceptable if three shells are used. Apart from reducing the computational effort, it should also be noted that the same dimensionless stress kernels  $M_{ijk}$  can be used at all lump levels provided the factor  $g$  in Equation (1) is made to corre-

Minimum lump separation, L	Maximum lump separation, 2L	Number of influences per iteration
1	2	$0,18 \times 10^6$
2	4	$0,50 \times 10^6$
3	6	$0,99 \times 10^6$
No lumping	-	$16 \times 10^6$

spond to the lump size. Furthermore, the influence range is limited by the lump shell parameter  $L$  as shown in Table 1. For example, if three-shell lumping is used, then kernel influences separated by more than six lump units from the receiving lump are never required.

The implications of this are that all influences can be stored in a fixed size kernel table, avoiding repetitive kernel computation or storage of kernels on comparatively slow mass storage. It can further be shown that kernel symmetries necessitate that only the positive  $X, Y, Z$  octant be stored.

The kernel storage table size is therefore given by

$$V = [2(L + 1)]^2 KH \quad (22)$$

where  $K$  is the number of kernel types (nine for stress kernels,  $M_{ijk}$ , and five for displacement kernels,  $N_{ijk}$ ) and  $H$  is the number of 'layers', parallel to the  $X, Y$  plane, in the  $Z$  direction. For example, the MINSIM-D solution program employs three-shell lumping,  $L = 3$ , and  $H = 31$  layers in the kernel table, requiring a memory allocation of  $8^2 \times 9 \times 31 = 17\ 856$  positions which can be accommodated readily in the main memory of most mini or micro computers.

The stored kernel arrangement is a particular feature of MINSIM-D and contributes to

the efficient determination of influences between arbitrarily oriented mined windows.

### Multiple reef solutions and scaling

Mining is often carried out on several reef horizons, and individual reef planes are invariably disturbed by faults and dykes. In addition, the determination of the amount of slip which can occur on a plane of weakness is of great importance when assessing potential rockburst hazards.

A specific design objective of MINSIM-D has been to allow the analysis of multiple reef mining problems. Each problem is considered to comprise a set of  $\eta$  windows which are oriented to cover the mining areas of interest. Slip on fault planes can be solved by locating fully mined windows with zero stope width over the areas of potential movement and by specifying appropriate sliding friction parameters.

The solution strategy is to solve each of the  $\eta$  windows in turn. Prior to the solution of the current window, the external stress influences  $\bar{E}_x$ ,  $\bar{E}_y$ ,  $\bar{E}_z$  due to the most recently estimated movements on all other windows are computed at each element of the window, using the stored kernel table and lumping techniques. The current window solution is then iterated to a specified tolerance and stored on disk. The maximum residual error occurring during iteration of each window is saved and compared to a specified tolerance after the solutions on all  $\eta$  windows have been updated. The entire cycle is then repeated until convergence is achieved.

In practice, the number of cycles is found to be dependent on the proximity of mined areas in different windows. Thus loosely coupled windows are usually solved in fewer than 5 cycles whereas extensive and closely overlapped reef planes may require up to 200 cycles. The piecewise constant nature of

the displacement discontinuity elements also limits parallel overlapped areas of mining to be separated by a minimum distance of one element.

This solution method may be adapted to allow 'scaling' of the solution values in areas of special interest. The problem solution is accomplished in two stages. In the first stage each window is solved with a 'coarse' element grid size of  $g$  (see Figure 1). All solutions are saved on mass storage. In the second stage 'fine' windows, with element grid sizes of  $g/4$ , are located within the coarse windows. Stress influences from all mined elements external to the fine windows are computed and used as boundary conditions for the solution of the set of fine windows. This technique provides a fourfold increase in scale resolution in the areas of interest, which coupled with the increases in resolution provided by partially mined elements, furnishes sufficient accuracy for the solution of almost all mining problems of interest in practice.

### Shallow depth problems

In order to maintain the convenience of the stored kernel table, shallow depth problems are solved by approximating the free surface as a single  $64 \times 64$  mined window rather than by introducing special kernel functions. The element grid size of the surface window is chosen to ensure that the window spans a surface area which is sufficiently extensive to cover all significant induced movement.

The surface window is incorporated in the overall solution cycle described previously. The external induced stresses arising on the surface plane, due to all other excavations, are computed as for any other window. The displacement discontinuity solution which corresponds to these stresses is, however, found directly by applying a

set of inverse kernels which can be inferred from the classical Boussinesq solution for a loaded half-space.

This method of treating shallow depth problems works satisfactorily although the surface displacements are not as smooth as those obtained by using appropriate half-space kernels. A limitation on mined windows is that they may not be located at a depth which is shallower than the grid size of a surface element.

### System structure

The MINSIM-D system consists of the five programs shown in Figure 4. The DIGITIZER capture program is used to create a digital representation of a mine plan outline. The FRONT-END program uses the outline to produce the inputs required by the SOLUTION and BENCHMARK programs, which are the core programs of the system. The SOLUTION program implements the solution techniques described, to solve the system of equations

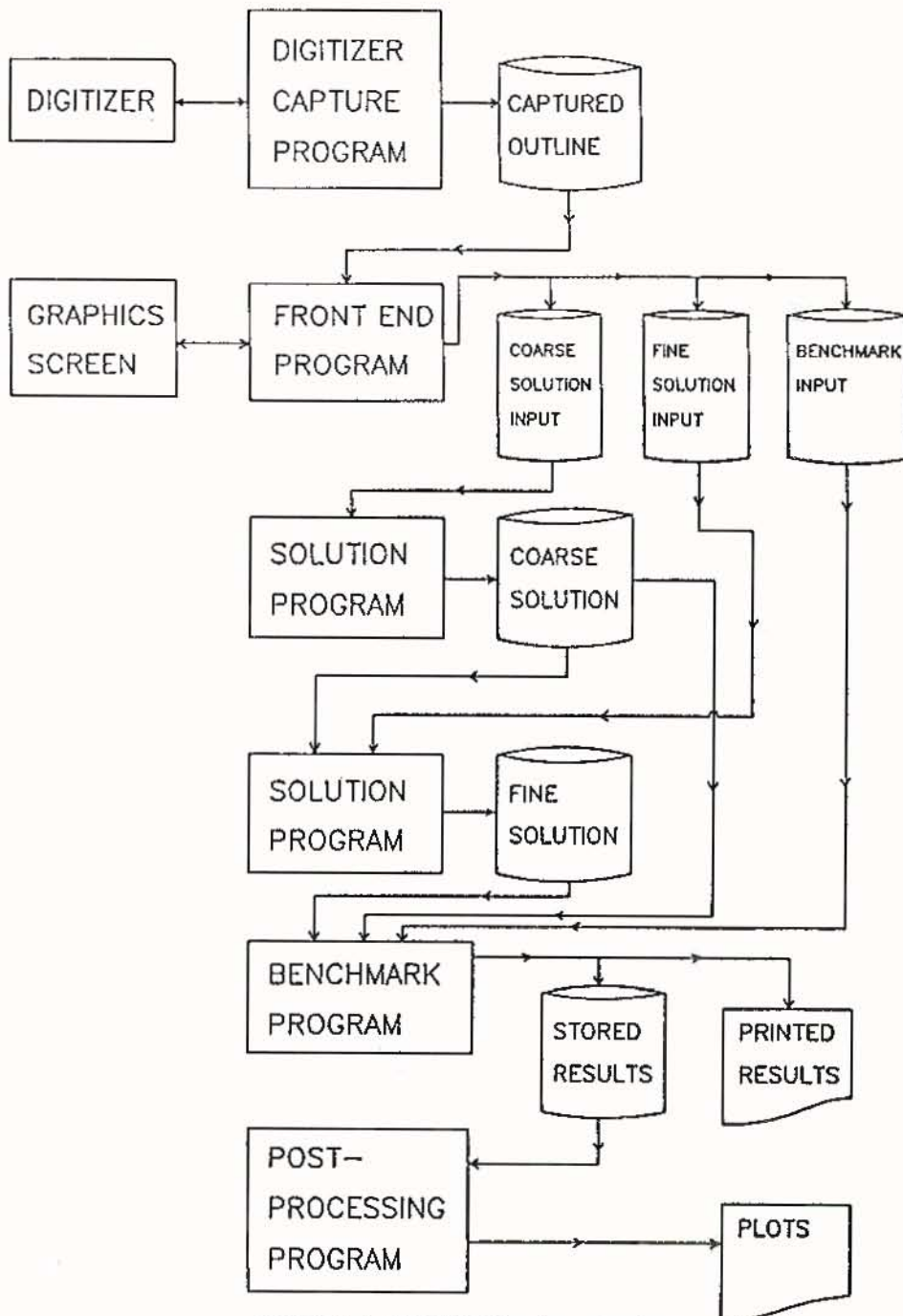


FIGURE 4. MINSIM-D system structure

for rides and convergences. The BENCHMARK program produces printed or plotted results on user defined planes called 'sheets'. The POST-PROCESSING program graphs the results obtained from the BENCHMARK program.

### Problem preparation

The input required by the SOLUTION program comprises elastic constants, the virgin stress field description and the excavation geometry. The geometry is described by planar square areas called windows. Each window consists of a grid of 64 rows and 64

columns of square elements. Each element is assigned a fraction-mined value, denoted by a single character code. A mined out element can be filled by backfill material or by yielding seam material. Windows can be used to model tabular reef excavations or fault planes.

Earlier versions of MINSIM required the user to enter a code for each grid element of each window. This was an arduous and error-prone task. The present system allows the user to capture and store mine plan outlines and at a later stage, to superimpose windows on these outlines. Generation of

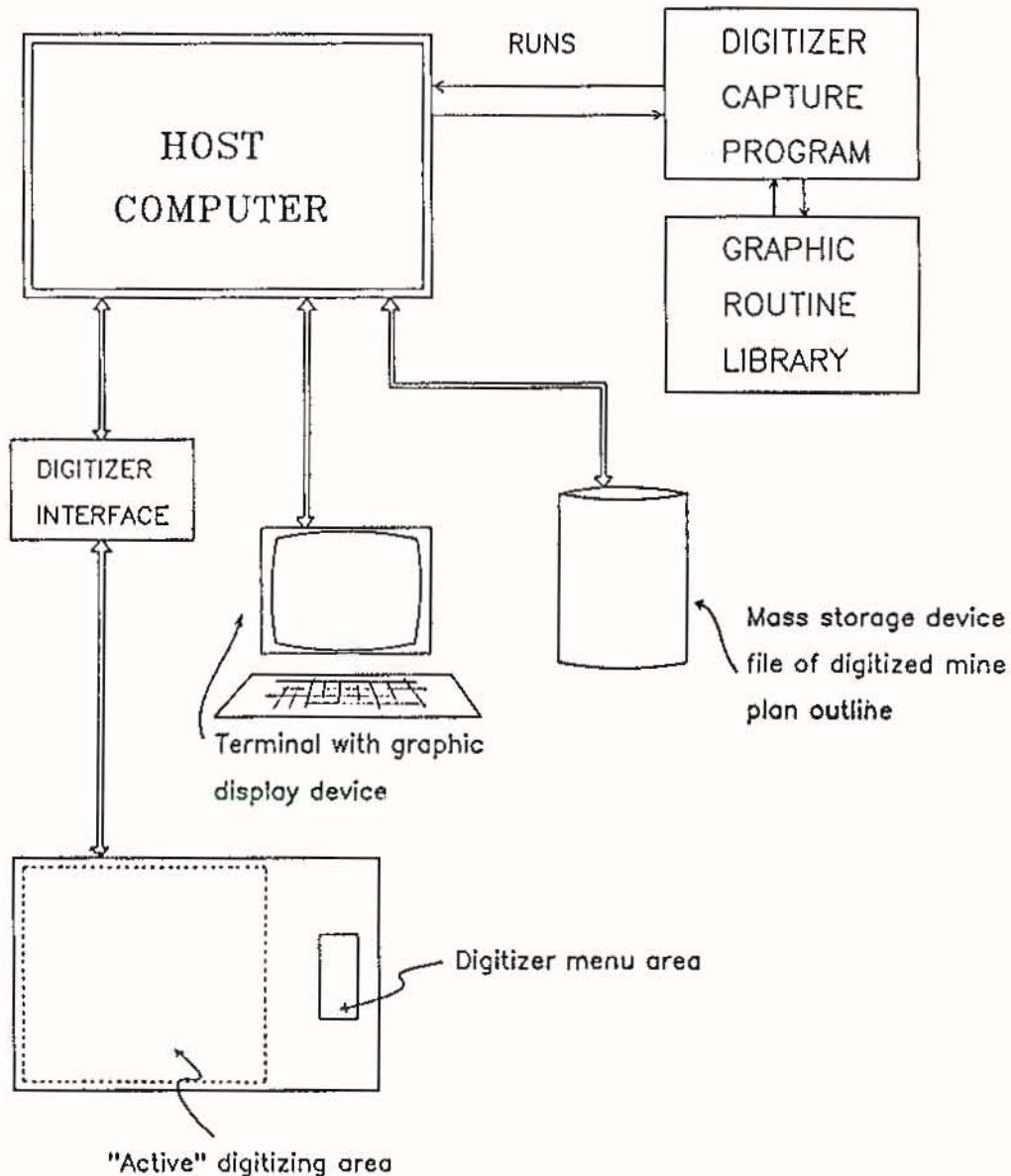


FIGURE 5. Hardware/software organization of the DIGITIZER program

the fraction-mined codes is carried out automatically.

### **The DIGITIZER capture program**

The hardware needed to run this program is shown in Figure 5. The host computer running the capture program can be a personal computer. The program is interactive, the graphic display being used to confirm that the digital representation is correct.

The data structure used to represent the mine plans is a linked list of line segments or 'chains'. A chain comprises a header entry which contains pointers to a linked list of coordinate pairs and to a table of exit branch pointers. The coordinate pairs are the digitized points representing the outline, and the exit branch pointers link the chain to other chains. The exit branch pointers contain date information, so that a link only becomes active at a certain 'mining step'. This structure allows a date to be associated with each excavation boundary that is digitized.

The chain header also identifies the reef plane containing the chain and the chain 'type'. The chain type indicates whether the line segment is a boundary between mined and unmined zones or between mined and back-filled zones.

### **The FRONT-END program**

The FRONT-END program can run on a mini or a personal computer. The user interactively supplies the elastic constant data, back-fill material descriptions, virgin stress state and position and orientation of windows. In addition the user can supply data for the benchmark program. A graphic feature of the program allows the user to display the locations of defined windows and benchmark 'sheets' superimposed on the mine plan outline.

The program generates window grid codes for a particular mining step and produces

the formatted input data files used by the SOLUTION and BENCHMARK programs. If the DIGITIZER and FRONT-END programs are run on a personal computer, these files can easily be transferred to a 'mainframe' computer. The SOLUTION and BENCHMARK programs are run in 'batch' mode, i.e. no user interaction is required. If mining step runs are done, the sequencing of the runs is left to the user. In addition to being able to vary the mine outline from one mine step to another, it is also possible to change the number of windows. This is useful in modelling slip on fault planes.

### **Output processing**

The SOLUTION program does not produce user requested results; this is done by the BENCHMARK program. The user can specify rectangular planes of interest, called 'sheets', which can be positioned anywhere in the elastic continuum. Specifically, sheets can overlay windows so that 'on-reef' results can be computed; alternatively sheets can intersect or lie parallel to windows for 'off-reef' results. A sheet is specified by the position of its origin and the orientation of its edges. The sheet size is given in terms of the number of points in each row and column and the row and column spacing. Results are computed at all the sheet points.

The user can select the variables of interest for each sheet. These variables reflect the state of stress at the sheet points. The user selects variables from a list of about ninety pre-defined possible values which include stress tensor components, principal stresses, failure criteria and strain and displacement components. The BENCHMARK program has been designed so that extension of the list of pre-defined variables is easily implemented. 'Standard' selections of the most commonly required

variables, such as principal stresses, displacement components and energy release rate, are available.

Output can be printed in tabular form or as 'character plot' representations of benchmark contours. The character plot contour range is computed automatically in rounded intervals.

A POST-PROCESSING program can be used to produce graphic contour and 'carpet' plots (these are three dimensional surface plots of contours).

### Illustrative case study

The following example briefly illustrates the use of the MINSIM-D system. The study

determines the excess shear stress on a fault plane separating two reef planes. The mine plan used is shown in Figure 6. This shows two reefs with different strike and dip angles, separated by a fault with a throw of about 100 metres. The outline was digitized from a single mine plan and stored as two reef planes, 'REEF1' and 'REEF2', in one output file.

Using the FRONT-END program, two windows, 'RF1' and 'RF2', were located on REEF1 and REEF2 respectively. A benchmark sheet was positioned over the central portion of the fault. The graphic display of the plan projection of the window and sheet positions is shown in Figure 7. The broken line rectan-

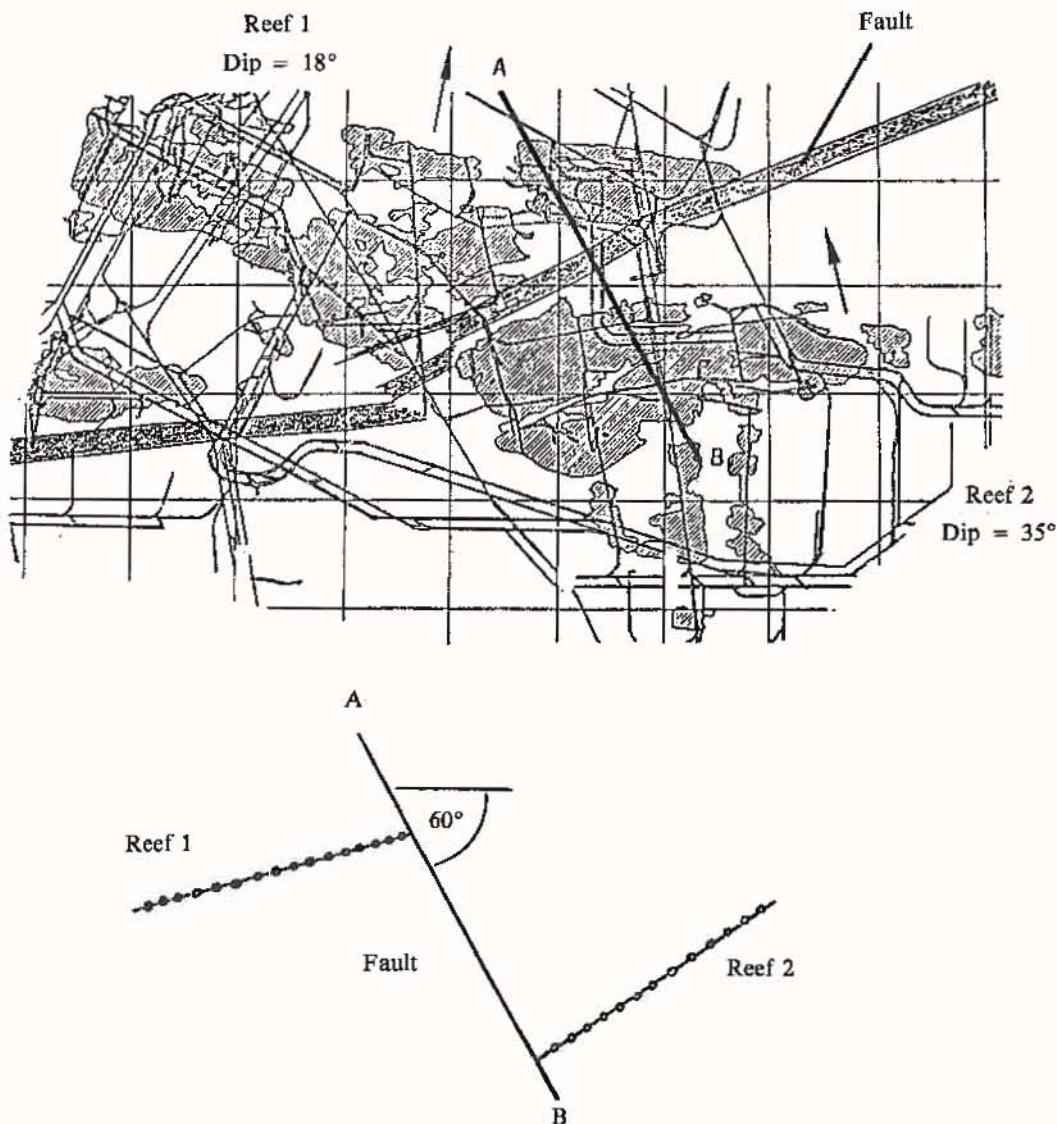


FIGURE 6. CASE STUDY — Plan view and section of displaced reef planes adjacent to a fault .

gle shows the edge of the sheet (fore-shortened by the projection). The solid line rectangles show the windows with identifying markers at their top left corners. Different line types are used to distinguish the different reefs. The window grid element size is 20 metres on edge.

The SOLUTION and BENCHMARK programs were then run on the data prepared by the FRONT-END. Figure 8 shows a character plot of a particular benchmark variable, the 'Excess Shear Stress' on the fault plane. Positive excess shear stress zones have been highlighted and indicate the areas on the fault plane which have a potential for slip. Reef intersections with the sheet are shown.

### Applications of MINSIM-D

MINSIM programs are used traditionally to design stoping sequences and layouts which reduce difficult mining conditions by minimizing design criteria such as the 'Energy Release Rate'.<sup>(14)</sup> In addition, the program is used routinely to evaluate potential low-stress sites for service excavations such as pump chambers, refrigeration plant chambers and haulages.

Examples of MINSIM-D applications which have been documented include a study of combined stabilizing pillars and backfill layouts, which was carried out to develop general guidelines for the design of regional support systems at great depths.<sup>(15)</sup> Another application has been the appraisal

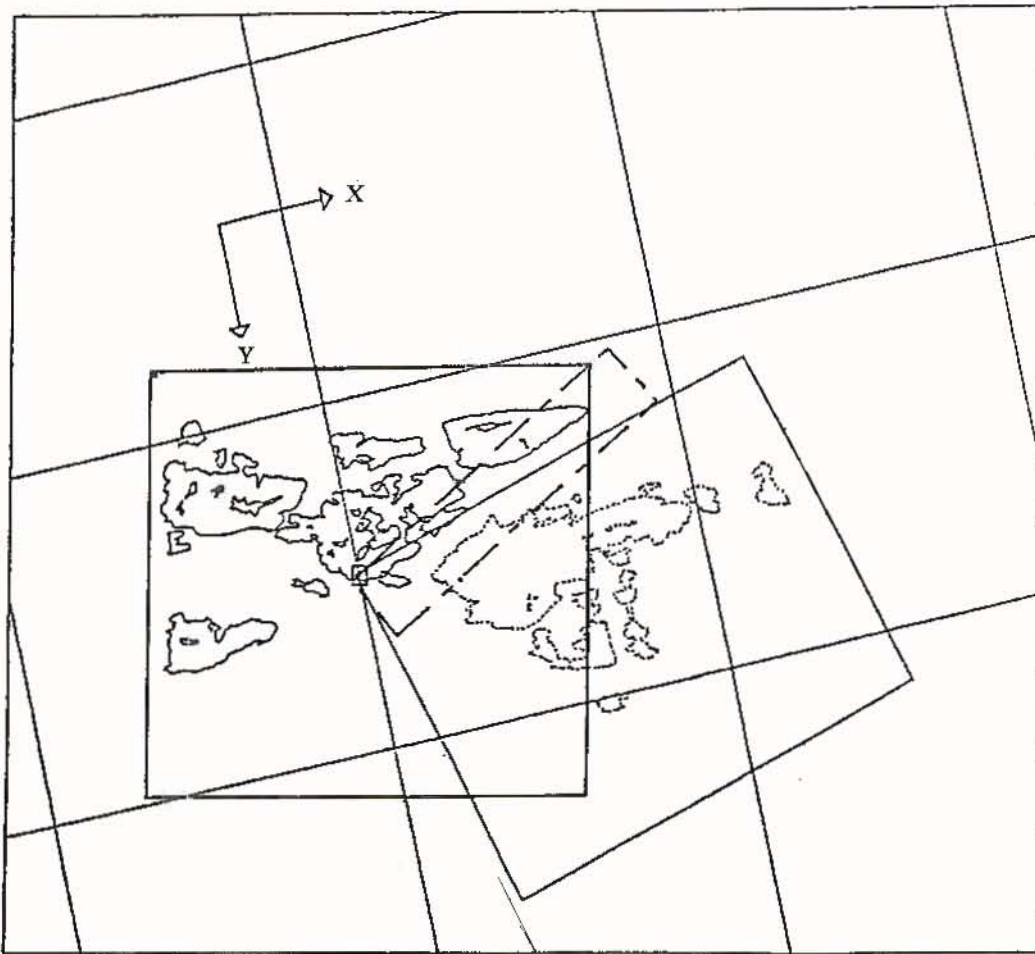


FIGURE 7. CASE STUDY — FRONT-END program display of coarse windows and a benchmark sheet superimposed on mining outlines

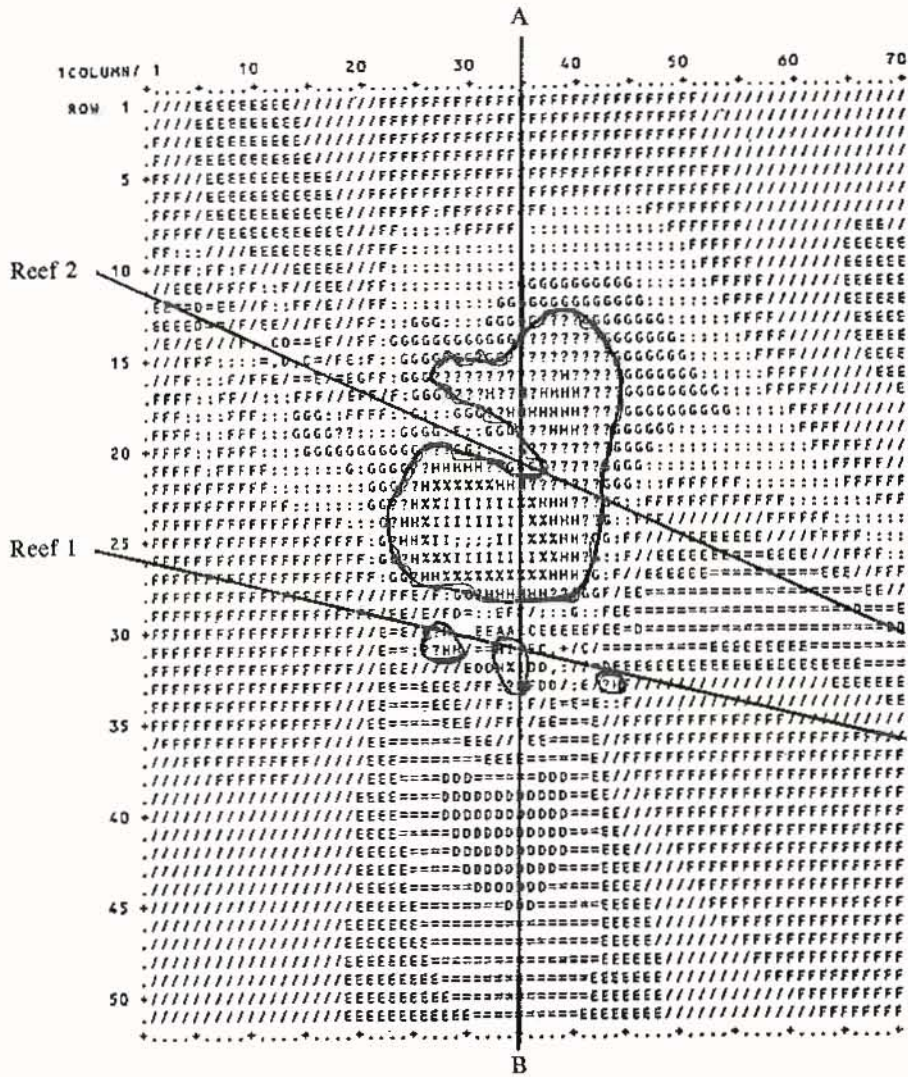


FIGURE 8. CASE STUDY — Character plot of positive excess shear stress zones on the fault plane

of some novel methods for the protection of vertical shaft systems. One such method is to extract the area in the vicinity of the shaft-reef intersection at the beginning of the shaft life.<sup>(16)</sup> This has the advantage of providing stress relief for the shaft service excavations at great depth but implies that lateral and vertical dislocations are created in the shaft at the reef intersection. The size of these dislocations can be controlled by appropriate installation of backfill material. The time dependence of the dislocation magnitudes can be found by modelling the extraction sequence during the shaft life.

A further problem of considerable importance is to locate benchmark sheets on planes

of weakness to evaluate measures of slip propensity such as Excess Shear Stress (ESS).<sup>(17)</sup> Movement on these planes can be estimated by placing a fully mined window, having zero stope width and suitable friction angle, on the fault plane and solving for the equilibrium rides. These can in turn be used to estimate the moment and magnitudes of possible seismic events generated on the fault plane.<sup>(18)</sup>

### Future developments

MINSIM-D has proved to be a robust tool for the solution of many tabular mine design problems, but there are inevitably a number of limitations to the present system. In particular, difficulties have been experi-

enced in transporting the SOLUTION and BENCHMARK programs to micro computers, although versions of the DIGITIZER and FRONT-END programs have been successfully adapted for micro computers.

A significant challenge, however, lies in developing multiple reef solution techniques which are considerably faster than those in use at present. This is required to circumvent the inherent limitations of smaller computers as well as to provide a more rapid interaction with the design engineer using the system. Particular attention is being given to improving the performance of lumping methods and to investigating alternative iteration strategies.

Additional investigations are currently being made into methods for modelling extensively faulted or undulating deposits with higher order elements, more realistic representation of the effects of non-linear rock behaviour near the stope face and modelling of bed separation effects close to mined areas. Further topics include the simulation of joint dilatancy as slip proceeds and the development of seam elements which are appropriate for representing the flexural and lateral interaction of thin-layer inhomogeneities such as dykes or sills.

### Conclusions

MINSIM-D is used extensively for the analysis and design of tabular layout problems in the South African gold mining industry but, to date, has been much less widely used for coal mining applications. The most important features of the system are the ability to model the interactions arising from mining on multiple horizons and slip on weak fault planes. MINSIM-D also provides capabilities for modelling 'soft' seam materials as well as backfill materials having hyperbolic or quadratic reaction characteristics. In addition a

fraction-mined attribute can be assigned to individual elements thereby increasing accuracy and resolution of complicated layouts. Sequences of mining steps can be specified to analyse incremental changes.

To assist the analyst in problem preparation, two special-purpose programs have been included in the MINSIM-D suite. The DIGITIZER program allows mining face positions to be transcribed directly from mine plans and stored as a digitized outline file. Incremental mining steps can be digitized and added to this file. The FRONT-END program allows the user to locate window outlines over areas of interest and generates automatically the window grids corresponding to the stored mining outlines. Both the DIGITIZER and FRONT-END programs can be run on mini or personal computers.

Particular attention has been given to the flexible reporting and analysis of solution results. Rockmass conditions can be evaluated at sets of field points arranged in rectangular 'sheets' which are arbitrarily located and oriented. This organization facilitates the production of synoptic contour diagrams in the form of either line printer character plots or as graphic contours.

### Acknowledgements

This paper describes work carried out as part of the research programme of the Research Organization of the Chamber of Mines of South Africa. Permission to publish this paper is gratefully acknowledged.

### References

1. ORTLEPP, W.D. and NICOLL, A. The elastic analysis of observed strata movement by means of an electrical analogue. J.S. Afr. Inst. Min. Metall., vol.65, 1965.

2. SALAMON, M.D.G. Elastic analysis of displacements and stresses induced by the mining of seam or reef deposits. J.S. Afr. Inst. Min. Metall., vol.64, Part I, 1963. pp. 128-149.
3. RONGVED, L. Dislocation over a bounded plane area in an infinite solid. J. Appl. Mech., vol.24, 1957. pp. 252-254.
4. CROUCH, S.L. Solution of plane elasticity problems by the displacement discontinuity method. Int. J. Num. Methods Engrng., vol.10, 1976. pp. 301-343.
5. SALAMON, M.D.G., RYDER, J.A. and ORTLEPP, W.D. An analogue solution for determining the elastic response of strata surrounding tabular mining excavations. J.S. Afr. Inst. Min. Metall., vol.64, 1964. pp. 115-137.
6. PLEWMAN, R.P., DEIST, F.H. and ORTLEPP, W.D. The development and application of a digital computer method for the solution of strata control problems. J.S. Afr. Inst. Min. Metall. vol.70, 1969. pp. 33-44.
7. DEIST, F.H., GEORGIADIS, E. and MORIS, J.P.E. Computer applications in rock mechanics. Application of Computer Methods in the Mineral Industry, 10th International Symposium, Johannesburg 1972.
8. BRIDGES, M.C., DAVIDSON, D., DUNCAN-FAMA, M.E. and FRIDAY, R.G. Application of the 'Displacement Discontinuity' technique to modelling of underground coal mining. Proceedings of the Fifth International Conference on Numerical Methods in Geomechanics.
9. MORIS, J.P.E. and ORAVECZ, K.I. Theoretical background to the development of a computer code for the modelling of seam-like deposits. Proceedings of the 26th US Symposium on Rock Mechanics. Rapid City, SD 1985. pp. 927-936.
10. DEIRING, J.A.C. An improved method for the determination, by a MINSIM type of analysis, of stresses and displacements around tabular excavations. J.S. Afr. Inst. Min. Metall., vol.81, 1980. pp. 425-430.
11. PEIRCE, A.P. and RYDER, J.A. Extended boundary element methods in the modelling of brittle rock behaviour. Fifth International Congress on Rock Mechanics, Melbourne, 1983. pp. F159-F167.
12. SALAMON, M.D.G. Elastic analysis of displacements and stresses induced by the mining of seam or reef deposits. J.S. Afr. Inst. Min. Metall., vol.65, Part IV, 1964. pp. 319-338.
13. RYDER, J.A. and NAPIER, J.A.L. Error analysis and design of a large-scale tabular mining stress analyser. Proceedings of the Fifth International Conference on Numerical Methods in Geomechanics. Nagoya 1985. pp. 1549-1555.
14. COOK, N.E.W., HOEK, E., PRETORIUS, J.P.G., ORTLEPP, W.D. and SALAMON, M.D.G. Rock mechanics applied to the study of rockbursts. J.S. Afr. Inst. Min. Metall., vol. 66, 1966. p. 493.
15. PIPER, P.S. and RYDER, J.A. An assess-

Nagoya 1985.

- ment of backfill for regional support in deep mines. Symposium on Backfilling in Gold Mines. MINTEK, Randburg, 1986.
16. MCKINNON, S.D. Alternatives to shaft pillars for the protection of deep vertical shaft systems. Paper to be published at Sixth International Congress on Rock Mechanics, Montreal, 1987.
17. RYDER, J.A. Excess shear stress assessment of geologically hazardous situations. Colloquium on Mining in the Vicinity of Geological and Hazardous Structures. MINTEK, Randburg, 1986.
18. NAPIER, J.A.L. Application of excess shear stress concepts to the design of mine layouts. Colloquium on Mining in the Vicinity of Geological and Hazardous Structures. MINTEK, Randburg, 1986.